The internal structure of modern barchan dunes of the Ebro River Delta (Spain) from ground penetrating radar

D. Gómez-Ortiz*, T. Martín-Crespo, I. Rodríguez, M.J. Sánchez, I. Montoya

Área de Geología, Dpto. de Biología y Geología, ESCET, Universidad Rey Juan Carlos, C/Tulipán s/n, 28933 Móstoles (Madrid), Spain.

* Corresponding author

E-mail: david.gomez@urjc.es

Tel.: +34 91 488 70 92

Fax: +34 91 664 74 90

Abstract

Ground penetrating radar is a non-invasive technique that allows the study of the structure of dune systems when outcrops are limited or protected. GPR response of sand dunes of the Holocene aeolian dunes of the Ebro River Delta (Spain) has been analyzed in this study in order to: characterise their internal architecture, determine their development and recent evolution, and calculate electromagnetic (EM) waves mean velocities in fine-grained sedimentary deposits. Several GPR profiles carried out in different representative areas have revealed the existence of different reflector packages that are related to differences in barchan-type dune activity. The area with a highest sand movement activity is characterized by small dunes, with overlapping reflector packages exhibiting reflections which dip up to 25º. When dune activity is moderate, dunes are higher (up to 5 m height) and their internal structure shows low-angle dip reflections except for the avalanche face, where dips up to 22º are identified. The area with the lowest sand movement, nearest to the coast line, is represented by small dunes with internal geometry consisting of partially overlapping elongated reflector packages defined by subhorizontal reflections. In all cases, a reflection associated to the location of the water table has been recognized at about 0.7 m depth. The results obtained from the GPR survey have allowed us to improve our knowledge about the dynamics of the coastal dune field and its relative evolution. They have shown that the morphology and geometry of the dune bodies adapt themselves to wind conditions, which permits the construction of coastal dune development models in order to establish the evolution of dunes.

Keywords: *Ground penetrating radar, Aeolian dunes, Ebro River Delta, internal structure*

1. Introduction

The GPR technique provides a unique insight into the internal structure of dunes which is not achieved by any other non-destructive geophysical technique. GPR has been used to examine the internal structures of aeolian sedimentary deposits such as ancient sand dunes (Harari, 1996) and more recently, Holocene dunes and dunefields (Bristow et al. 2000 and 2005; Bristow and Pucillo 2006; Pedersen and Clemmensen 2005; Costas et al. 2006; Heggy et al. 2006). GPR response of sand dunes of aeolian origin has been analyzed in this study in order to: characterize their internal architecture, determine their development and recent evolution, and calculate electromagnetic (EM) waves mean velocities in fine-grained sedimentary deposits.

2. Geological setting

This study has been carried out in the Ebro River Delta, formed by a sand dune field superimposed on the typical delta scenario where the river deposits have been re-worked and re-distributed by the sea currents defining its actual coast line. The dynamic balance between the excess supply of stream-borne sediments and waves, coastal currents and tides, is determinant in shaping a river mouth and its deltaic plain. The Ebro River Delta is located along the northeast coast of the Iberian Peninsula, 170 km from Barcelona (Fig. 1). The Holocene deposits of the delta have a thickness ranging from 18 m on the landward side of the delta to 51 m at the delta front.

Morphologically, the Ebro Delta has two spits closing two lagoons: El Fangar, located in the NW, and Los Alfaques, located in the SW and linked to the main delta body through the Trabucador bar. The Fangar spit, where the dunes of this study are located, is nearly 6 km long, with a maximum width of 1.4 km in the middle part, and spreads north-westward forming a bay. The outermost part of the delta consists of a long dune system which represents the longest and the only active dune system of the Delta (Rodríguez et al. 2003). The dimensions of the dune system are variable depending on the wind and tidal conditions. Currently, its present length is about 5 km (Serra et al. 1997).

The dune system of El Fangar has been divided in four zones based on dune activity: Zone 1, with the highest activity, is located in the northern part; Zones 2 and 3 site in the intermediate zone, and contain dunes of larger size, this being the reason why they exhibit the smallest movement and, Zone 4, which is located in the southern part, is similar to Zone 1, but with lower activity. Dune morphologies are: barchan in Zones 1 and 4, and barchanoid ridges in Zone 2 and 3. This distribution is related both to the orientation of the coast and to the predominant direction of the highest intensity winds blowing from 315º. A typical cross-section of the internal structure of barchan dunes with labeled surfaces is shown in figure 2. Wind and migration directions are also depicted in order to compare with the obtained GPR stratigraphy.

This study has a special relevance because the dune system of El Fangar spit has never been studied with this technique, as The Ebro Delta is a Natural Park, with restricted access. GPR is a non-destructive method to identify subsurface structure without the use of trenches (Bristow et al. 2000), thus representing one of the best methods to investigate the ground in protected areas.

3. Ground penetrating radar (GPR)

As GPR is a well-established geophysical method (Davis and Annan 1989; Telford et al. 1990; Daniels 1996; Reynolds 1997; Claerbout 2004), only a brief overview of it is presented here. The technique is based on the measurements of the subsurface response to high frequency (typically 100-1000 MHz) electromagnetic (EM) waves. A transmitting antenna on the ground surface emits EM waves in distinct pulses into the ground that propagate, reflect and/or diffract at interfaces where the dielectric permittivity of the subsurface changes. EM wave velocity data thus allows conversion of a time record of reflections into an estimated depth.

3.1. Data collection and presentation

Data from this study were collected with the Subsurface Interface Radar (SIR) 3000 system developed by Geophysical Survey Systems, Inc. (GSSI). GPR measurements were made using a 200 MHz centre frequency shielded antenna in monostatic mode, which is considered as the best compromise between penetration depth and event resolution in sedimentary materials (Jol et al. 2003). All the profiles have been collected in continuous mode, with a distance interval between traces of 0.1 m and a total number of 1024 samples per scan. The topography along the profile was obtained by means of a differential GPS and the data were used to correct the topography in the data processing. In this continuous acquisition mode, each trace of the radargram is the result of a 64 times stacking in order to improve the signal-to-noise ratio. A survey wheel attachment was used in order to enhance survey accuracy. Automatic gain control was employed during data acquisition and depending on dune height, a time window of 50 or 100 ns two way travel time (TWT) was applied.

Following the scheme proposed by Neal (2004), data processing comprised zero-time corrections, signal-saturation corrections, automatic gain control (AGC), band-pass filtering, static corrections, and Kirchoff migration. Although published data for EM wave velocities in sedimentary materials are available, each specific study area displays particular dielectric features, due to specific inherent heterogeneities of each of its sedimentary lithologies. For this reason, calibration surveys were necessary in order to obtain a mean EM wave velocity value applicable to all profiles, so that a representative dielectric constant could be calculated. The calibration survey was carried out over a representative zone of the area, where a metallic bar had been horizontally introduced. From this calibration survey, and given that the depth of the point source (the metallic bar) was well known (0.77 m), and the reflections were perfectly recognizable in the obtained radargram, a mean velocity of 0.15 m•ns^{-1} was estimated. In addition, a independent velocity estimation was performed by determining the velocity value that better fitted the geometry of the hyperbolic reflection caused by the metallic bar (Fig. 3). In this case, a 0.16 m•ns^{-1} mean velocity was obtained. Therefore, we can conclude that a velocity interval of 0.15–0.16 m•ns^{-1} can be taken as representative of the materials in this area. These values are very similar to those published by different authors (e.g. Smith and Jol 1992; Reynolds 1997; Costas et al. 2006) for dry sand, which range from 0.12 m•ns^{-1} to 0.17 m•ns^{-1}. Taking into account the mean EM wave velocity obtained from the calibration survey, a maximum depth of 7.5 m could be reached employing a time window of 100 ns for data acquisition. It must be pointed out that the estimated velocity is only valid for the sand material located above the water table, due to the fact that wet sand exhibits lower velocity values, as is well known. As the time windows were determined in order to study mainly the unsaturated zone, we consider that the obtained velocity value is valid for depth determination. Once the velocity data were obtained, a migration process was applied in order to collapse the diffraction hyperbolae and obtain true geometries and depths of the subsurface structures along the profiles. All data were processed, modelled and interpreted using the software REFLEXW 3.5. In all profiles, the position of the antennae is represented on the horizontal axis, whereas depth is depicted with no scale exaggeration on the vertical one.

4. Results and interpretation

During the field survey, 14 GPR profiles with a total length of 1120 m were carried out. The location of profiles was planned in such a way that they covered all the different types of coastal dunes present in the study area. A summary of the GPR performance in the study area is displayed in Table 1. For the sake of brevity, only five representative profiles (Fig. 4) have been selected in this work.

As the coastal dunes exhibit heights ranging from 1 to 5 m, two different time windows were selected: 50 ns for the smaller dunes and 100 ns for the larger ones. In all cases, the other acquisition parameters remained the same, as well as the topography data collection method. As a general statement, GPR profiles exhibit a good signal-to-noise ratio in the whole time window. In addition to this, all GPR profiles show a much higher intensity at the central part, corresponding to the coastal dunes, than at the edges, where water saturated sands are predominant. Moreover, a reflection located at a very constant depth of about 0.7 m can be seen in all the profiles, although under the dune formations it is obscured by other reflections. From direct field observations made at small trenches, the 0.7 m depth reflection can be associated to the location of the water table. Conductive saline groundwater increases attenuation below the water table. In addition to this, deeper reflections are multiples of the air and ground waves at the top of the profile. For these reasons, the profiles have not been interpreted below the water table except where attenuation is low.

In order to obtain information about the internal structure of the sand dunes, several GPR profiles were carried out in both transverse and longitudinal orientations to the different dune types. In this work, 5 GPR profiles are shown: two of them are transverse to small (< 1 m height over the surrounding plain) dunes (Zones 1 and 3), two more profiles are transverse to higher (> 4 m height over the surrounding plain) dunes and one profile is longitudinal to one of the previous highest dunes (Zone 2). In all cases, different units can be identified in the radargrams, based on the different reflector packages exhibited by the reflections and the cross-cutting relationships between them. In this sense, we have used the concept of radar sequence analysis (Beres and Haeni, 1991; Gawthorpe et al., 1993) that defines the radar sequences boundaries by picking at reflection terminations. The location of the reflection associated to the water table is also shown. A detailed explanation of each profile is given below, including labelling of the main internal stratification features for comparison with a simple barchan dune (Fig. 2). Although we have described four different morphodynamics zones, we only consider here three of them because the results obtained in two continuous zones (2 and 3) were very similar. Thus, we only take into account three zones from now on.

4.1. Zone 1 – profile 1

It corresponds to a 58 m long GPR profile (Fig. 5) carried out over a small barchan-type dune (about 24 m in length) located at the NW part of the study area, near the position of the calibration profile. It exhibits a slightly asymmetrical transverse profile shape and its maximum height over the surrounding plain is about 1 m. Due to the small size, a 50 ns time window was chosen. A reflection located at a TWT of about 40 ns corresponds to the position of the water table. The intensity of the reflections is much greater in the interior of the dune than in the surrounding plain constituted by sands with a higher water content that attenuates the signal.

A complex internal structure is defined by the different reflections present at the interior of the dune, making difficult to locate the location of the water table due to the intensity of the reflections. Three different reflector packages can be identified in the profile. The first one corresponds to the reflections located between 18 and 28 m in the horizontal distance and a TWT from 30 to 50 ns. This unit exhibits reflections with a poorly defined structure but with a general convex-upward shape. It has been interpreted as a protodune that acted as a nucleation site for the actual dune. Immediately above this unit, a sharp contact (B in Fig. 5) defines a second one that can be identified between 14 and 30 m of horizontal distance. Inside this unit, reflections showing a mean dip of about 25º SE can be clearly defined (E in Fig. 5). It seems that this unit has been developed over the previous one and thus, the reflections have been adapted to the previous palaeotopography. A sharp contact, located between 26 and 30 m in the horizontal distance, is recognized between this unit and the third one (B in Fig. 5), the latter extending as far as 41 m from the beginning of the profile. The reflections located inside this third unit dip similar to the second unit (about 25º SE) but flatten as we move towards the SE, resulting in nearly horizontal reflections. This can be interpreted as resulting from a period of time where the wind energy decayed and the vertical accretion of the dune was dominant, in contrast with the reflections of the second unit, that would imply higher wind energy and a lateral migration of the dune towards the SE.

4.2. Zone 2 – profiles 2 and 3

Profile 2 consists of a 71 m long GPR profile (Fig. 6) over a large barchan-type dune (about 44 m length) located at the central part of the study area (Fig. 4). Its transverse profile shape is clearly asymmetric, and its maximum height is about 4 m over the surrounding plain. In this case, and due to the vertical dimension of the dune, a 100 ns time window was chosen. As in the previous profile, a reflection located at a TWT of about 70 ns corresponds to the position of the water table.

Although at a first glance the internal structure of the dune seems to be quite simple, three different units can be distinguished. The first one extends from the beginning of the dune (18 m in the horizontal distance) to 48 m in the upper part of the dune and 56 m in the lower one. It consists of parallel reflections describing a convex-upward geometry with some local cross-cuttings relationships. These relationships can be clearly seen between 32 and 40 m in the horizontal distance, and at a depth of about 1 to 2 m below the ground surface. There are some, short SE dipping reflections intersecting the stronger reflections that describe the general arched geometry of the dune (E in Fig. 6). This kind of geometry has been previously described in different works (e.g. Pye and Tsoar 1990; Bristow et al. 2000; Pedersen and Clemmensen 2005) and is normally interpreted as evidence of lateral migration of the dune due to the wind. Over this unit a sharp boundary (B in Fig. 6), defining a new one, can be identified between 48 and 62 m in the horizontal distance. This second unit is defined by reflections dipping about 22º towards the SE and partially overlapping the reflections of the previous unit (A in Fig. 6). This structure can be interpreted as dune avalanche foresets. A small, third unit is also present in the slipface of the dune, ranging from 52 to 60 m in the horizontal distance and with a thickness lower than 0.5 m. It is defined by a small flat-topped wedge that seems to partially overlap the previous unit. Although its thickness is too small to reveal any internal structure using the 200 Mhz antenna, the geometry of the reflection that defines its upper bound is clearly overlapping the upper reflection of the second unit. Thus, this third unit can be interpreted as the deposit resulting from a small avalanche of the windward face of the dune.

Profile 3, a 245 m long longitudinal GPR profile (Fig. 7), was carried out in the same dune in order to study its internal structure in a direction normal to the direction of propagation of the dune. The reflection located at 70 ns TWT and related to the position of the water table, is also present and it seems to be more continuous than in the transverse profile 2. A clear attenuation in the signal can be observed below this reflection due to the high water content, although the internal structure of the dune remains visible below it.

Comparison between the longitudinal and transverse profiles, shows that internal structures in each direction are completely different. At least six distinctive units are visible along the radargram, based on the cross-cutting relationships of the reflections (B in Fig. 7). Each unit is defined by a certain number of parallel reflections describing undulating geometries. The largest one is located at the base of the dune, and extends from about 10 to 200 m in the horizontal distance.

On top of that basal unit, four small units (e.g. D in Fig. 7) can be recognized along the profile. The reflections inside these units partially overlap the ones of the basal unit, indicating that they are younger, and are interpreted as the deposits related to the dune migration. This indicates that, at a certain period of time, the dune can only be active in a restricted sector where deposition occurs. Each unit would represent sectors where the dune has been active in different periods of time, indicating several pulses of dune development. A small unit, extending from 200 to 220 m in the uppermost part of the dune and with a reduced thickness, is the only one that does not overlap the lower unit, but only the upper ones.

4.3. Zone 2 – profile 4

Profile 4 is an 85 m long GPR profile (Fig. 8) over a large barchan-type dune (about 64 m length) located within the central part of the study area (Fig. 4). The transverse profile is slightly asymmetric and its maximum height is about 3.2 m over the surrounding plain. As in the previous case (profiles 2 and 3) and due to the vertical dimension of the dune, a 100 ns time window was chosen. Again, a reflection located at a TWT of about 70 ns corresponds to the position of the water table, although it is hardly visible below the central part of the dune due to the reflections from its internal part.

Although this dune closely resembles the previous one in the field, its internal structure determined from the GPR data is quite different. Up to 5 different units can be determined, resulting in a more complex structure than that observed in Fig. 6. A first remarkable difference is that the profile shape of the dune is not very asymmetrical. Furthermore, the dune exhibits an initial 20 m long section with a nearly flat profile and a much reduced thickness. From 32 to 74 m of the radargram, the dune displays a more typical profile, similar to that of Fig. 6 dune.

Internally, the first unit is represented by the above described 20 m long section. It is characterized by reflections showing a low angle (A in Fig. 8), SE dip and cross-cutting relationships (e.g. at 12 and 22 m of the profile). The final part of this unit is overlapped by a new unit (B in Fig. 8) extending from 32 to 66 m in the horizontal distance. Its characteristics are subhorizontal reflections (A in Fig. 8) that locally exhibit low angle dip reflections (e.g. between 45 and 52 m) defining a SE sense of dune movement. This unit is overlapped by another new one, extending from 42 to 61 m at the upper surface of the dune, and showing subhorizontal reflections that reproduce the geometry of the upper boundary of the lower unit. Its thickness is small (about 1 m maximum) and it is partially overlapped (B in Fig. 8) by a new unit extending from 52 to 72 m, that constitutes the windward face of the dune. The reflections overlap the previous unit at a very low angle but its dip increases up to 20º towards the slipface of the dune (D in Fig. 8). Finally, and similar to what is seen in profile 2, a small unit with a thickness lower than 0.5 m is also present between 65 to 74 m in the horizontal distance. This unit has a similar flat-topped wedge geometry that seems to partially overlap the previous unit. It would correspond again to the deposit resulting from a small avalanche of the windward face of the dune.

4.4. Zone 3 – profile 5

Profile 5, a 95 m long GPR profile (Fig. 9), was carried out over two small barchan dunes (about 24 m length each) separated by a 12 m long interdune depression.

This profile is located at the south eastern part of the study area. The transverse profile shape of these dunes is strongly asymmetrical, but its maximum height over the surrounding plain is small (< 1.5 m). Due to the small vertical dimension of the dunes, a 50 ns time window was also selected in this case. The reflection corresponding to the position of the water table is then located at a TWT of about 50 ns, but its continuity below the central part of the dunes is difficult to establish due to the presence of other reflections.

The dunes exhibit a complex internal structure with several overlapping units defined by boundary surfaces (B in Fig. 9). The dune located towards the NW is defined by three units, whereas the one located towards the SE is composed by four units (e.g., D in Fig. 9). In general, all units belonging to both dunes are elongated in shape and are characterized by subhorizontal reflections that reproduce the geometry of the lower unit, generally increasing its dip towards the windward face of the dune (E in Fig. 9). In addition, a small unit occurs in the slipface of both dunes. In this case, the geometry is not elongated but wedge-shaped, with a flat top surface, and seems to be related with a certain avalanche process at the slipface. The presence of different partially overlapping units is interpreted as due to an active dune migration.

Dominant wind actions determine dune dynamics and their morphology (Lancaster, 1995). NW is the direction of the more frequent and strong winds in this area. Consequently, the sedimentary system response is to migrate to the SW (Sánchez et al., 2007). For each radargram, except for the longitudinal one, migration direction can be identified from the reflector dips and reactivation surfaces. Although all the sedimentary system moves to the SW, not all the dunes have the same migration rates; this depending upon the dune height (Bagnold, 1941). Zones 1 and 3 have lower dune heights than zone 2, and thus different morphodynamic conditions. This is the reason why the internal structure imaged in profiles 1 and 5 is more complex and chaotic than in profiles 2 and 4. Dunes with lower elevation are more rapidly destabilized and reconstructed than dunes with higher elevation. In addition, dunes of profile 5 are also affected by wave erosion during strong storms, and this contributes to their complex internal structure. In contrast, internal structures in profiles 2 and 4 are more homogeneous and organized.

5. Discussion

The aforementioned results and interpretations demonstrate the usefulness of the GPR technique for studying the internal structure of recent Aeolian dunes. However, it is well known that all the geophysical techniques have some limitations and this is not an exception. The main limitations encountered during this study correspond to the signal attenuations observed when the water table was located near the surface. In those cases, the attenuation makes the interpretation of the internal geometry of the dunes very difficult, due to the scarce information provided by the radargrams. In this sense, using different antennae with different frequencies could help to minimize this effect. For example, the combination of a 200 Mhz central frequency antenna with a 100 Mhz one, could help to obtain greater penetration depths, although the expected signal attenuation would be similar. In contrast, the use of a 400 Mhz central frequency antenna could have been useful to obtain more vertical resolution but its penetration depth would have been lower. So, the use of a 200 Mhz antenna is considered a good compromise between penetration depth and vertical resolution. In case a multichannel GPR system was available, it could have been useful in order to compare the information obtained using different antennae at the same time.

Regarding profile orientations, the maximum information is obtained when the profile is oriented parallel to the wind direction (i.e. transverse to the dune). If different profiles, taken at different angles (30 degrees, 45 degrees, etc) to the transverse or longitudinal profiles were carried out, the information would be essentially the same, except that the inclination of the reflector would be lower, exhibiting a minimum when the profile is oriented transverse to the wind direction (i.e., a longitudinal profile).

The use of longer step distances (e.g. 0.25 m or 1 m) during the data acquisition would provide similar results except for the detailed internal structure, due to the lower horizontal resolution. The depth to the water table as well as the geometry of the main sequences of reflector packages would be obtained independently of the horizontal data spacing but, the longer step distances, the scarcer information about the internal structure of these units. In this sense, a compromise between data spacing and the required detailed internal resolution for the study has to be established prior to data acquisition.

Comparing the different GPR reflector packages obtained in this study with other published GPR studies dealing with different types of dunes (e.g. Van Dam et al., 2003, star dunes; Bristow et al., 2000 and 2005, complex linear dunes; Pedersen and Clemmensen, 2005, parabolic dunes) we can conclude that they show substantial differences and thus, GPR profiles can be used in order to discriminate different dune types from a detailed interpretation of the observed sequences of reflector packages. However, some other questions related to morphodynamics of the dune system cannot be directly answered with a simple GPR survey and they would need a detailed and complete monitoring. For example, the study of the time span necessary for the imaged internal dune structures to form, or the role of the water table all through the dune formation process, would imply an exhaustive monitoring of the dune system that is beyond the scope of this work. Nevertheless, it would be interesting, as future work, to promote similar studies using the GPR technique in order to improve the knowledge about the morphodynamics of modern dune systems.

6. Conclusions

In this study, the internal structure of the dune field of El Fangar spit in the Ebro Delta, as well as the depth of the water table have been analysed. The wind direction and the sense of movement of the dunes have been determined in all profiles, based on the different shapes of migration obtained.

GPR profiles have revealed the existence of different radar sequences that are related to differences in barchan-type dune activity. In this way, small dunes with overlapping radar sequences characterize the area with a higher activity, whereas larger dunes (up to 5 m height) exhibiting internal structure with low-angle dip reflections, except for the avalanche face, are dominant when dune activity is moderate. The area with the lowest activity, nearest to the coast line, is represented by small dunes with internal geometry consisting of partially overlapping elongated radar sequences defined by subhorizontal reflections.

The water table has been recognized at about 0.7 m depth, and is defined by a reflection occurring in all profiles.

This considerably improves the knowledge of the dune field dynamics and its evolution, which will allow~~s~~ the future establishment of a correct *Integrated Coastal Zone Management.*

GPR technique has proven to be one of the best methods to analyze the internal structure of dunes, especially in protected or access restricted areas, like the Ebro Delta, as this is a non-invasive method.

Acknowledgments

We would like to thank the staff of the Natural Park of the Ebro Delta for permitting fieldwork in the area. This work is funded with the Project CGL-2005-04189, from The Ministry of Science and Technology of Spain. We wish to thank Dr Essam Heggy, Dr. Curt Peterson, an anonymous reviewer and the Editor for their constructive comments, which have greatly contributed to improve the manuscript.

References

Annan AP (1999) Practical Processing of GPR data. Sensors and Software. Ontario, Canada

Bagnold, R (1941) The physics of blown sand and desert dunes. London, Methuen, 265 p

Beres M, Haeni FP (1991) Application of ground-penetrating radar methods in hydrogeological studies. Ground Water 29: 375-386

Bristow CS, Chroston PN, Bailey SD (2000) The structure and development of foredunes on a locally prograding coast: insights from ground-penetrating radar surveys, Norfolk, UK. Sedimentology 47: 923-944

Bristow CS, Lancaster N, Duller GAT (2005) Combining ground penetrating radar surveys and optical dating to determine dune migration in Namibia. J Geol Soc London 162: 315-321

Bristow CS, Pucillo K (2006) Quantifying rates of coastal progradation from sediment volume using GPR and OSL: the Holocene fill of Guichen Bay, south-east South Australia. Sedimentology 53: 769–788

Claerbout JF (2004) Earth soundings analysis: Processing versus inversion. Blackwell Scientific Publications 3, Cambridge, UK

Costas S, Alejo I, Rial F, Lorenzo H, Nombela MA (2006) Cyclical evolution of a modern transgressive sand barrier in Northwestern Spain elucidated by GPR and aerial photos. J Sediment Res 76: 1077-1092

Daniels DJ (1996) Surface-Penetrating Radar. The Institution of Electrical Engineers, London, UK

Davis JL, Annan AP (1989) Ground-penetrating radar for high-resolution mapping of soil and rock stratigraphy. Geophys Prospect 37: 531-551

Gawthorpe RL, Collier RELI, Alexander J, Leeder M, Bridge JS (1993) Ground penetrating radar: application sandbody geometry and heterogeneity studies. In: Characterisation of fluvial and Aeolian reservoirs (Eds. CP North and DJ Prosser), Geol. Soc. London Spec. Publ. 73, 1128-1143

Harari Z (1996) Ground-penetrating radar (GPR) for imaging stratigraphic features and groundwater in sand dunes. J Appl Geophys 36: 43-52

Jol HM, Lawton DC, Smith DG (2003) Ground penetrating radar: 2-D and 3-D subsurface imaging of a coastal barrier spit, Long Beach, WA, USA. Geomorphology 53: 165-181

Lancaster, N (1995). Geomorphology of Desert Dunes. Routledge, London.

Neal A (2004) Ground-penetrating radar and its use in sedimentology: principles, problems and progress. Earth-Sci Rev 66: 261-330

Pedersen K, Clemmensen LB (2005) Unveiling past aeolian landscapes: A ground-penetrating radar survey of a Holocene coastal dunefield system, Thy, Denmark. Sediment Geol 177: 57-86

Pye, K and Tsoar, H (1990) Aeolian Sand and Sand Dunes, Unwin Hyman, London, 396 p

Reynolds JM (1997) An Introduction to Applied and Environmental Geophysics. John Wiley, New York, USA

Rodríguez, I, Galofré, J, Montoya, F (2003) El Fangar spit evolution. Coastal Engineering VI: Computer Modelling and Experimental Measurements of Seas and Coastal Regions. WIT PRESS, UK. 419-425

Sánchez MJ, Rodríguez I, Montoya I (in press) Short Term Coastal Dune Evolution of Fangar Spit (Ebro Delta). In: ICCD07 (eds.), International Conference on Management and Restoration of Coastal Dunes. Santander, Spain

Serra J, Riera G, Argullos J, Parente-Maia L (1997) El transporte eólico en el delta del Ebro: evaluación y contribución al modelado litoral. Boletin Geologico y Minero

108 (4-5), 477-485

Smith DG and Jol HM (1992) Ground penetrating radar results to infer depositional processes of coastal spits in large lakes. Geological Survey of Finland Special Paper 16, 169-177

Telford WM, Geldart LP, Sheriff RE (1990) Applied Geophysics. Cambridge University Press, 770 p

Van Dam, RL, Nichol, SL, Augustinus, PC, Parnell, KE, Hosking, PL McLean, R.F (2003) GPR stratigraphy of a large active dune on Parengarenga Sandspit, New Zealand. The Leading Edge 22(9), 865-870

Figure captions

Figure 1. Location map of the study area at the NE of the Iberian Peninsula.

Figure 2. Cross-section of the internal structure (A) and photograph (B) of a typical barchan dune (modified from Pye and Tsoar, 1990). A: Foresets; B: Bounding surfaces; C: Trough cross-bed set; D: Wedge-planar cross-bed set; E: Tabular-planar cross-bed set.

Figure 3. Radargram of the calibration survey and correlation with the location of the metallic bar into the dune. The Antenna (200 Mhz) and the survey wheel can be observed.

Figure 4. Digital Elevation Model (DEM) of the study area obtained during the field survey (September 2006). Solid lines represent the location of all the GPR profiles. The selected radargrams (dotted lines) are numbered and displayed more in detail within the three insets, corresponding to the differentiated zones.

Figure 5. Zone 1, profile 1: (A) Field photograph of the profile. (B) Processed and migrated radargram. (C) Interpretation of the radargram with the three different radar sequences identified in the profile (see text for details). Same labels as in figure 2.

Figure 6. Zone 2, profile 2: (A) Field photograph of the profile. (B) Processed and migrated radargram. (C) Interpretation of the radargram with three different units

distinguished. The first one (18 to 48 m) consists of parallel reflections describing a convex-upwards geometry with some local cross-cuttings relationships. Over this unit, a new one (48 to 62 m) is defined by reflections dipping about 22º towards the SE and partially overlapping the reflections of the previous unit. The third unit (52 to 60 m) is defined by a small flat-topped wedge that seems to partially overlap the previous unit. Same labels as in figure 2.

Figure 7. Zone 2, profile 3: (A) Field photograph of the profile. (B) Processed and migrated radargram. (C) Interpretation of the radargram with at least six distinctive units visible along the radargram, based on the cross-cutting relationships of the reflections. Each unit is defined by a certain number of parallel reflections describing undulating geometries (see text for details). Same labels as in figure 2.

Figure 8. Zone 2, profile 4: (A) Field photograph of the profile. (B) Processed and migrated radargram. (C) Interpretation of the radargram, where up to five different units can be determined (see text for details). Same labels as in figure 2.

Figure 9. Zone 3, profile 5: (A) Field photograph of the profile. (B) Processed and migrated radargram. (C) Interpretation of the radargram. The dune located towards the NW is defined by three units whereas the dune located towards the SE is composed by four units (see text for details). Same labels as in figure 2.

Figure 1

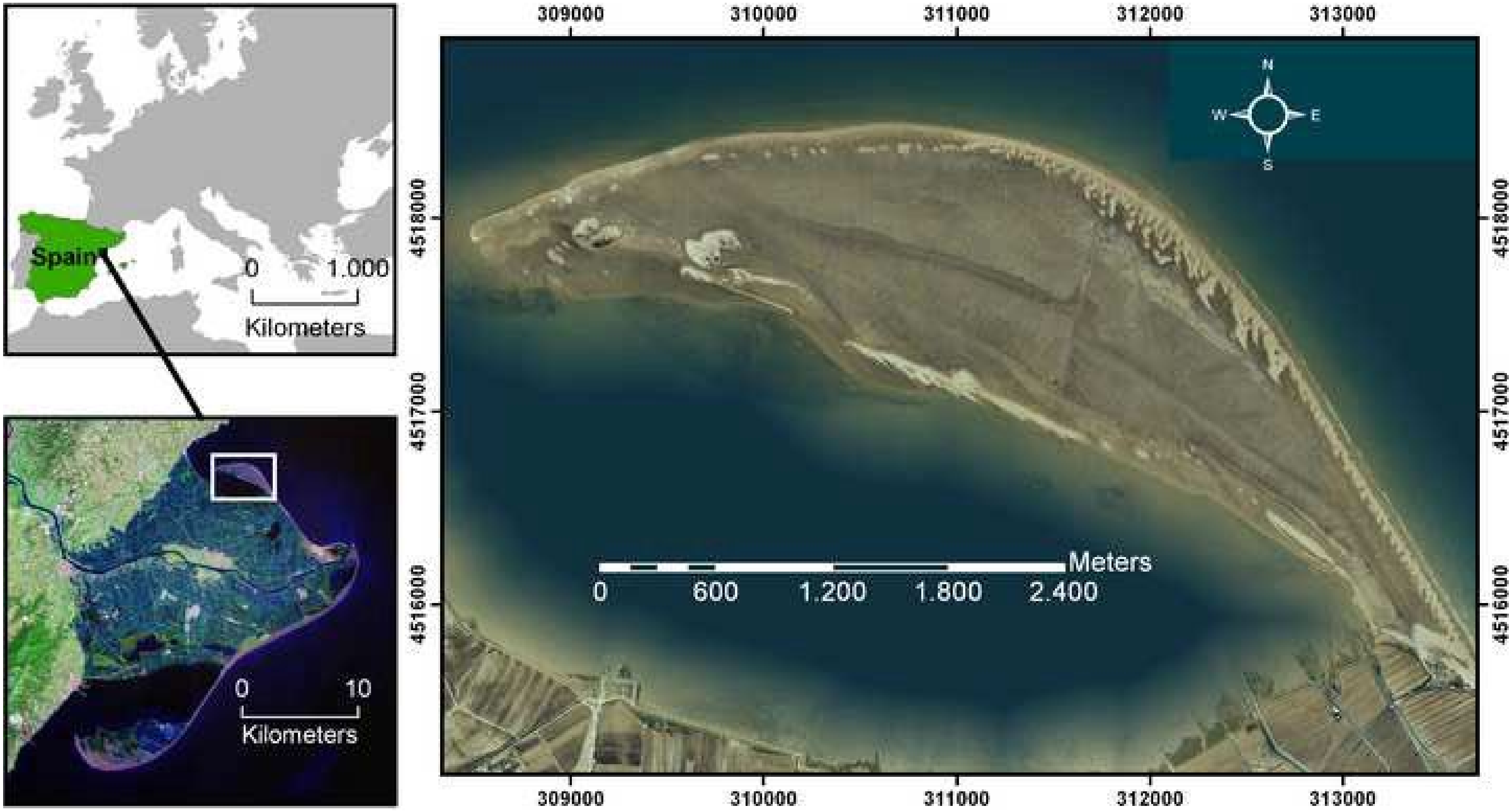
Spain
0
1.000
Kilometers
0
10
Kilometers
309000
310000
311000
312000
313000
4518000
4517000
4516000
N
W
E
S
Meters
0
600
1.200
1.800
2.400

Figure 2

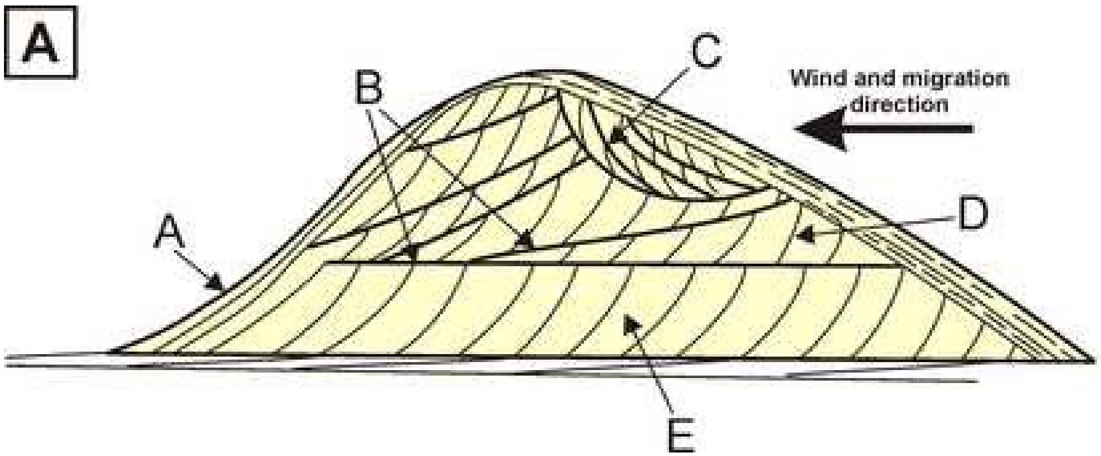

Figure 3

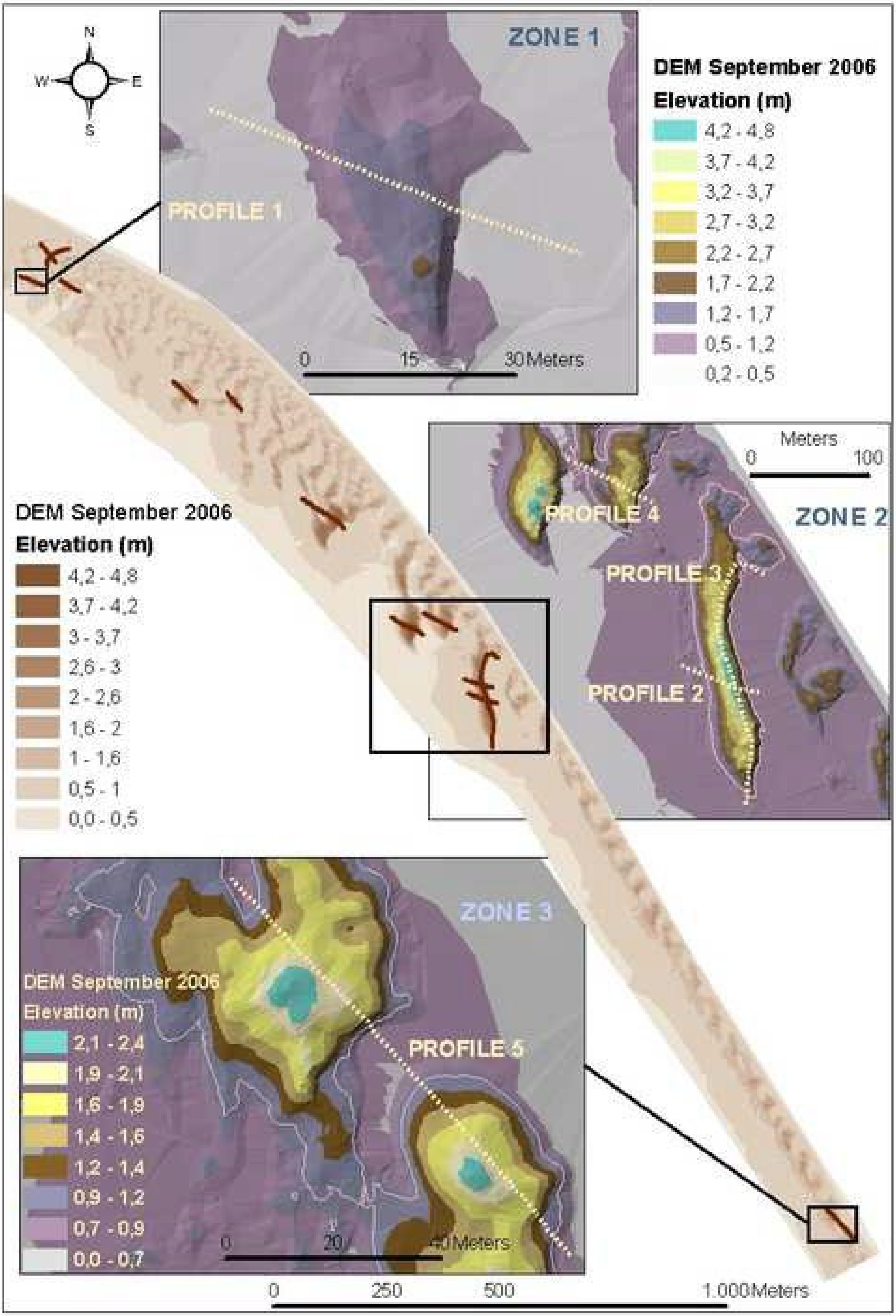
N
W
E
S
ZONE 1
DEM September 2006
Elevation (m)
4,2 - 4,8
3,7 - 4,2
3,2 - 3,7
2,7 - 3,2
2,2 - 2,7
1,7 - 2,2
1,2 - 1,7
0,5 - 1,2
0,2 - 0,5
PROFILE 1
0
15
30 Meters
Meters
0
100
PROFILE 4
ZONE 2
PROFILE 3
PROFILE 2
DEM September 2006
Elevation (m)
4,2 - 4,8
3,7 - 4,2
3 - 3,7
2,6 - 3
2 - 2,6
1,6 - 2
1 - 1,6
0,5 - 1
0,0 - 0,5
ZONE 3
DEM September 2006
Elevation (m)
2,1 - 2,4
1,9 - 2,1
1,6 - 1,9
1,4 - 1,6
1,2 - 1,4
0,9 - 1,2
0,7 - 0,9
0,0 - 0,7
PROFILE 5
0
20
40 Meters
0
250
500
1.000 Meters

Figure 4

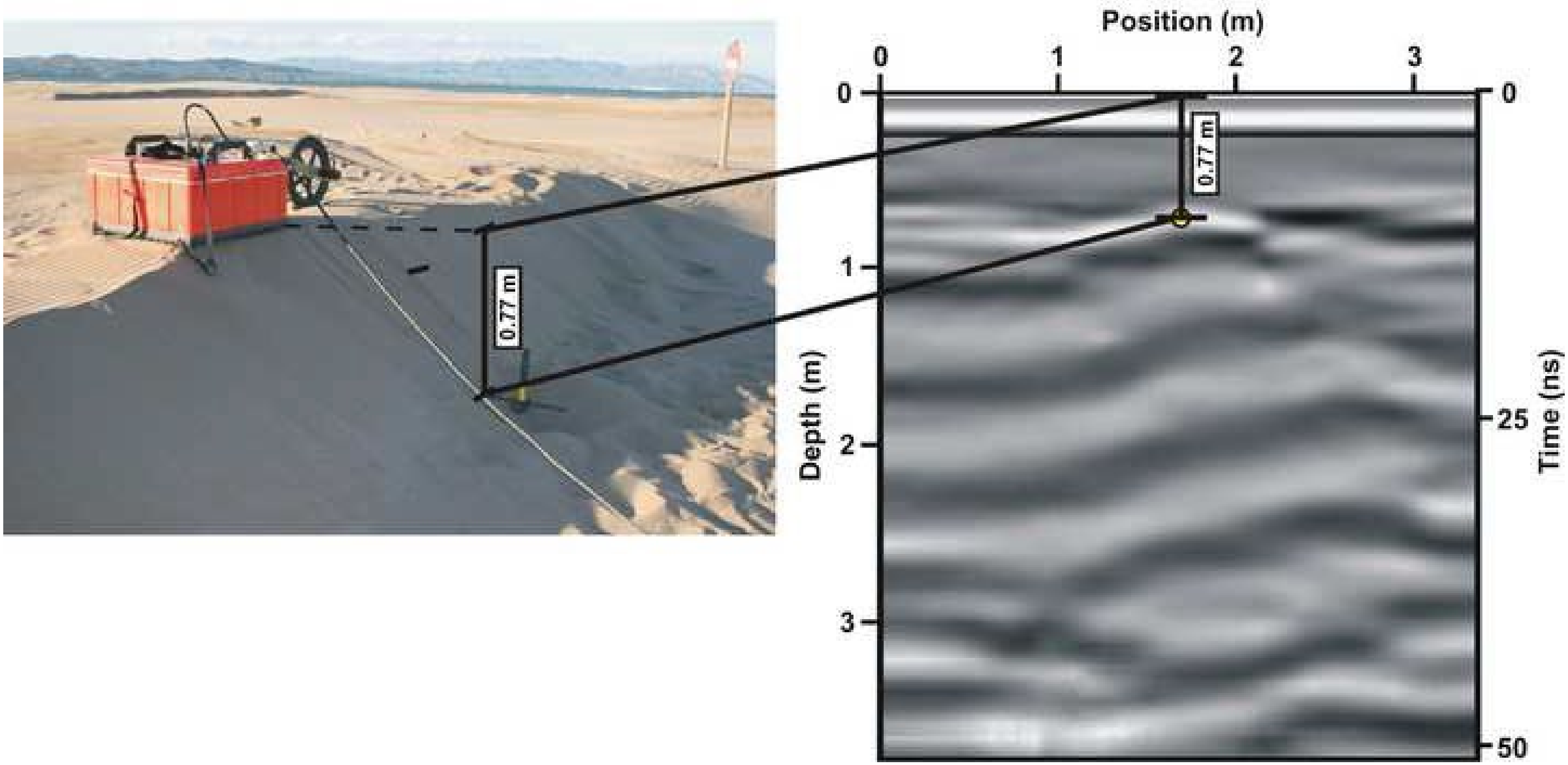

Figure 5

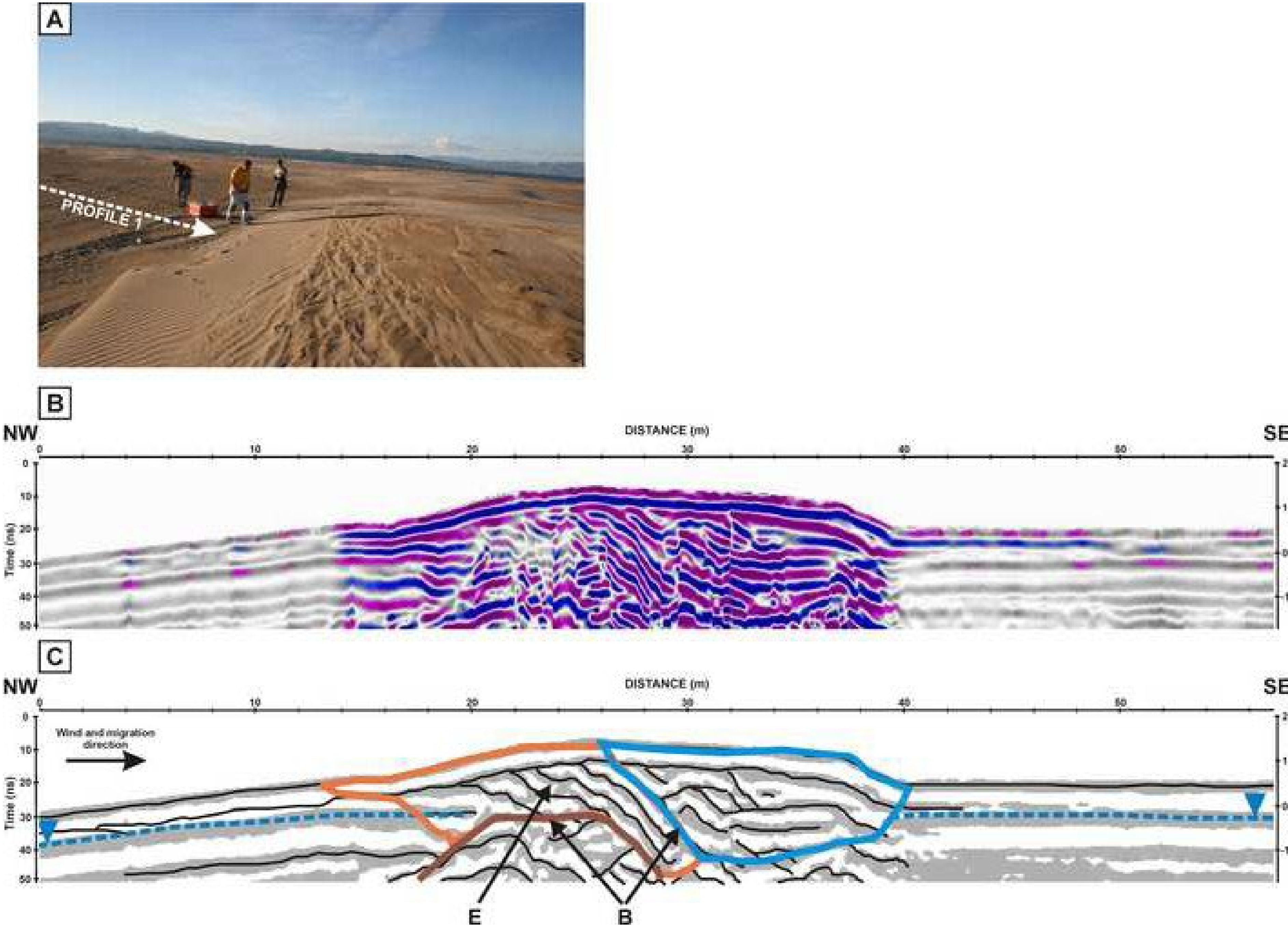
A
PROFILE 1
B
NW
SE
DISTANCE (m)
0
10
20
30
40
50
Time (ns)
Elevation (m)
C
Wind and migration direction
E
B

Figure 6

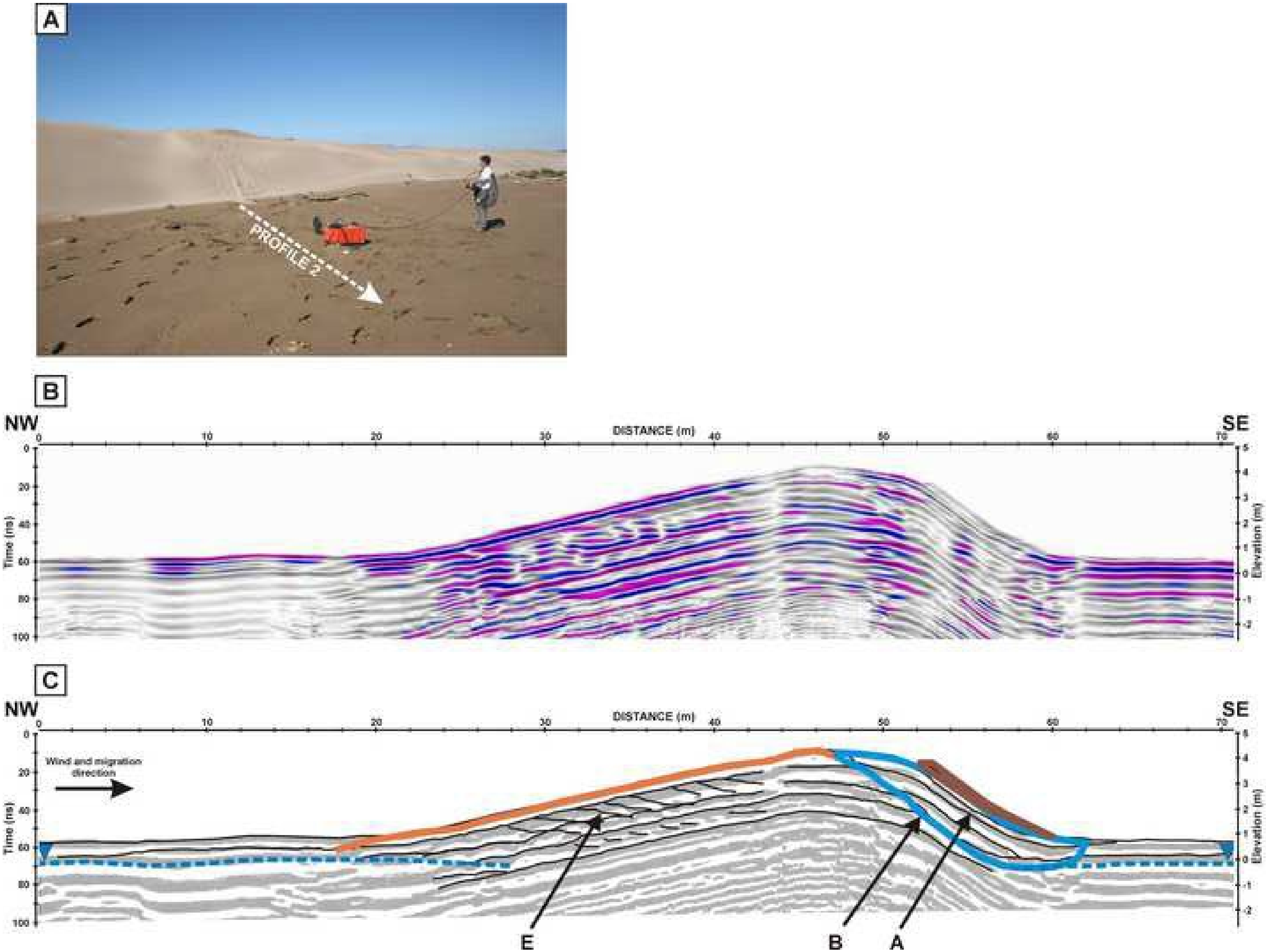
A
PROFILE 2
B
NW
SE
DISTANCE (m)
Time (ns)
Elevation (m)
C
NW
SE
DISTANCE (m)
Wind and migration direction
Time (ns)
Elevation (m)
E
B
A

Figure 7

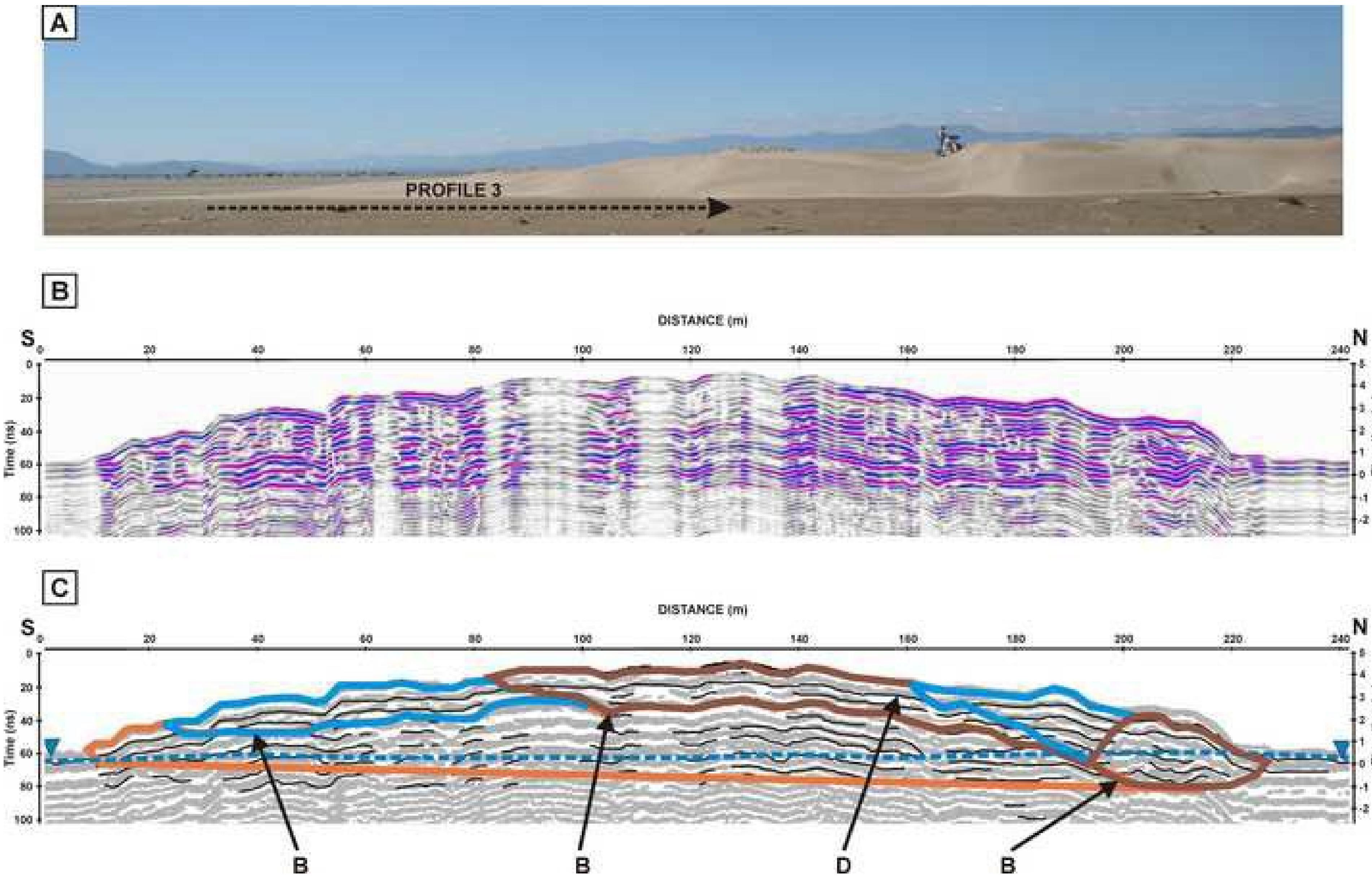
A
PROFILE 3
B
DISTANCE (m)
S
N
Time (ns)
Elevation (m)
C
DISTANCE (m)
S
N
Time (ns)
Elevation (m)
B
B
D
B

Figure 8

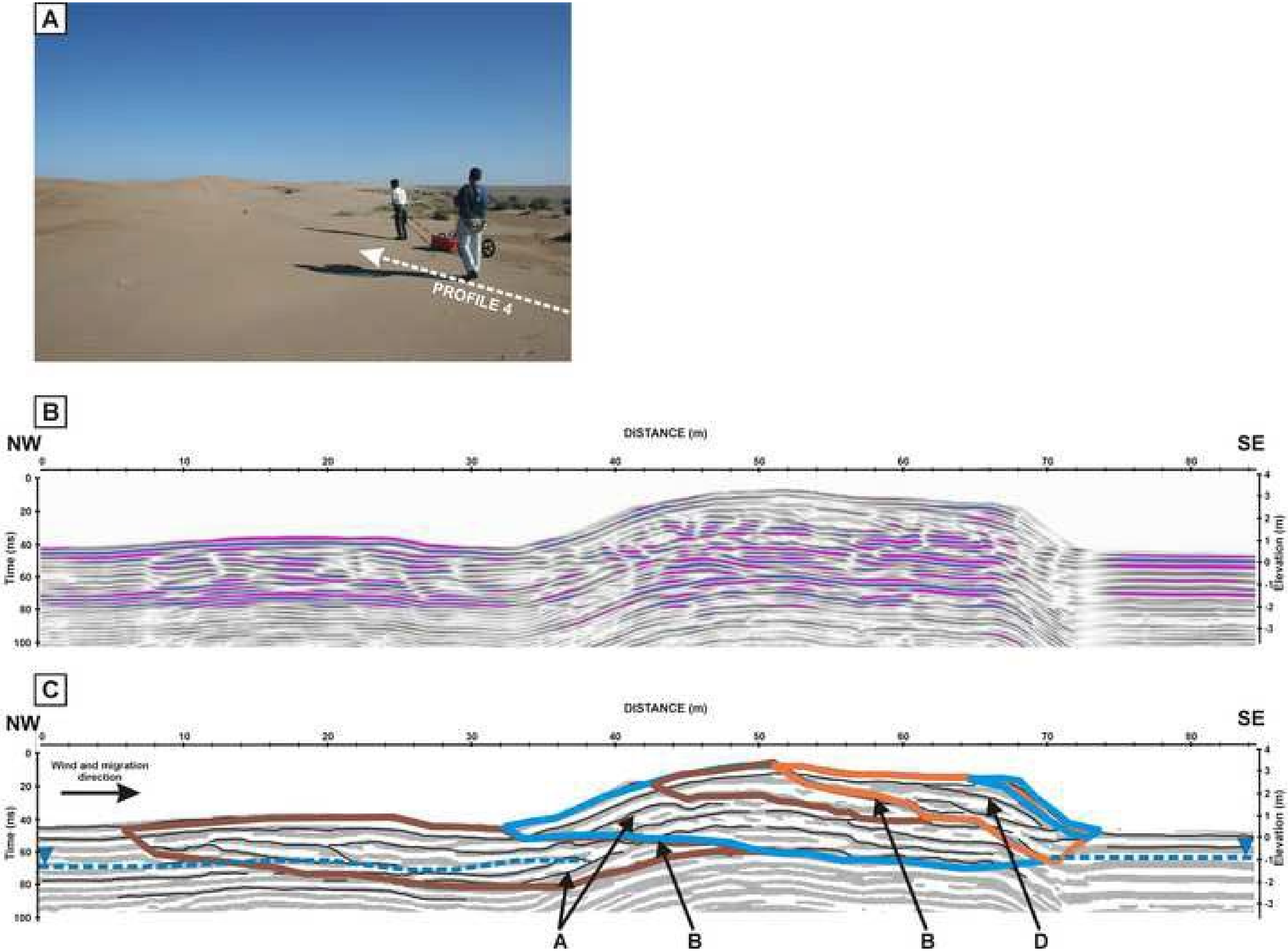
A
PROFILE 4
B
NW
SE
DISTANCE (m)
Time (ns)
Elevation (m)
C
Wind and migration direction
A
B
B
D

Figure 9

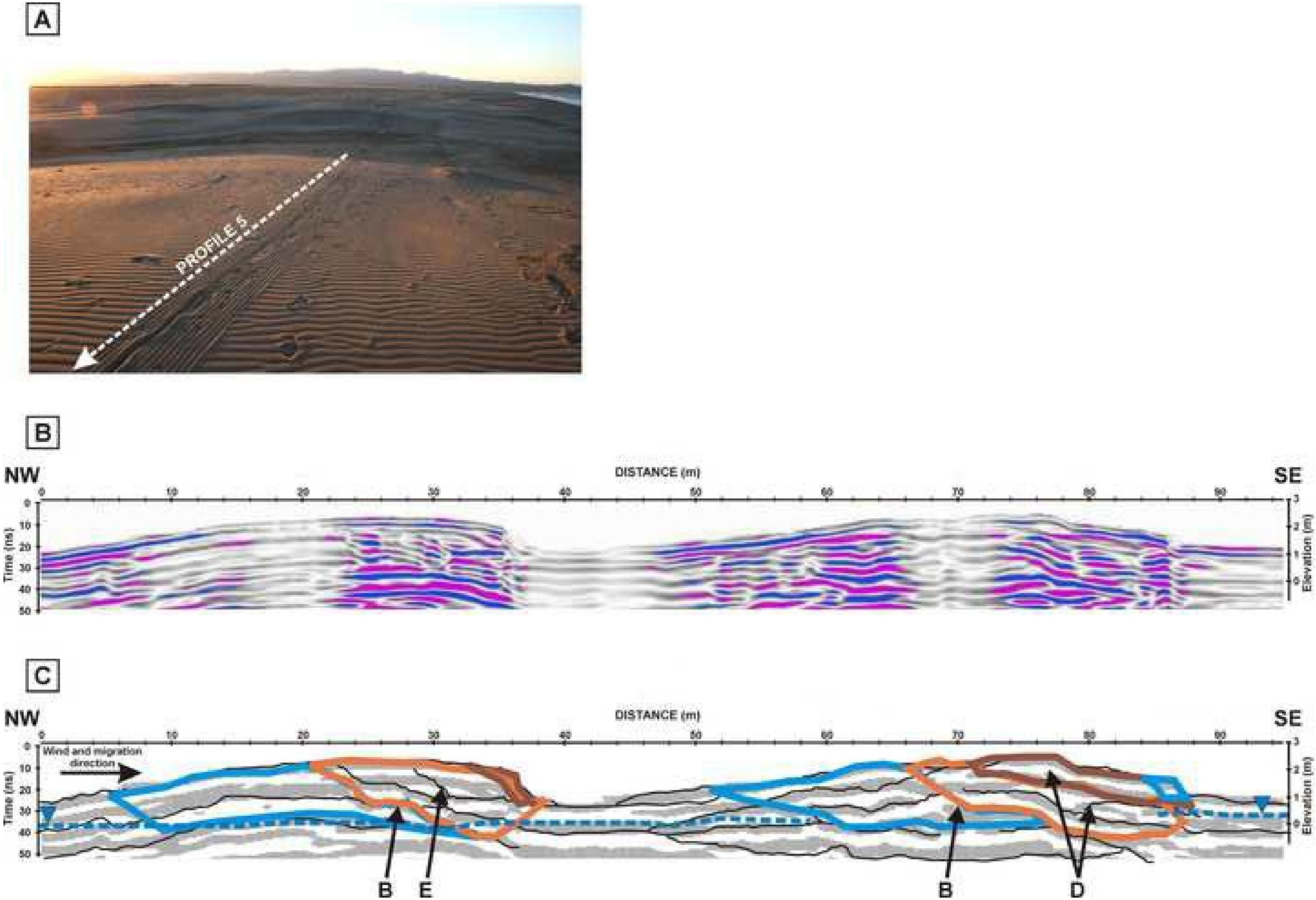
A
PROFILE 5
B
NW
DISTANCE (m)
SE
Time (ns)
Elevation (m)
C
NW
DISTANCE (m)
SE
Wind and migration direction
Time (ns)
Elevation (m)
B
E
B
D

Table 1

Velocity estimates	0.15–0.16 m•ns^{-1}
Penetration depth	3.75 m (50 ns TWT) to 7.5 m (100 ns TWT)
Horizontal resolution	0.1 m
Vertical resolution	0.097 ns
Groundwater influence	Groundwater table at 0.7 m depth. Moderate signal attenuation below the central part of the dunes. Strong signal attenuation at the outer parts of the profiles.